

Structure of multi-oxygen-related defects in erbium-implanted silicon

This article has been downloaded from IOPscience. Please scroll down to see the full text article.

2002 J. Phys.: Condens. Matter 14 8537

(<http://iopscience.iop.org/0953-8984/14/36/310>)

View [the table of contents for this issue](#), or go to the [journal homepage](#) for more

Download details:

IP Address: 171.66.16.96

The article was downloaded on 18/05/2010 at 14:56

Please note that [terms and conditions apply](#).

Structure of multi-oxygen-related defects in erbium-implanted silicon

J D Carey

School of Electronics, Computing and Mathematics, University of Surrey,
Guildford GU2 7XH, UK

E-mail: David.Carey@surrey.ac.uk

Received 13 May 2002, in final form 3 July 2002

Published 29 August 2002

Online at stacks.iop.org/JPhysCM/14/8537

Abstract

In a previous report, electron paramagnetic resonance measurements of erbium and oxygen implanted into silicon revealed centres with monoclinic and trigonal symmetry. These centres were tentatively ascribed to different atomic configurations of O and Si atoms surrounding a central Er^{3+} ion. In the light of recent calculations concerning the structure and stability of multi-oxygen-related defects in silicon, more sophisticated models have now been developed. The structure of the monoclinic centres observed is attributed to an Er atom sitting at the tetrahedral interstitial site surrounded by six O atoms. In this model the O atoms are arranged in the form of three O interstitial dimers with each of the O atoms located near to the Si–Si bond-centred positions. In the case of the prominent defect centre which exhibited trigonal symmetry, different possible structures for this centre are explored including locating the Er^{3+} ion residing at the hexagonal interstitial site surrounded by six O atoms as well as a centre consisting of an O-decorated ring hexavacancy defect.

1. Introduction

There is a growing realization of the importance of the role played by impurity- and defect-related complexes in understanding many of the electronic properties of silicon [1]. The study of the structure of multi-oxygen-related centres, in particular, has become important in recent times in the quest to understand the mechanism associated with the diffusion of O in Si [2]. Whilst it is generally accepted that single-interstitial oxygen (O_i) atoms are located near to the bond-centred (BC) position in the Si lattice forming two short ($\sim 1.6 \text{ \AA}$) Si–O bonds, the activation energy for diffusion of the O_i centre is too high to explain the aggregation of O in Si and the resultant generation rates associated with thermal donor defects [2, 3]. It has been proposed that multi-O centres, such as the O dimer (O_{2i}), behave as the fast diffusion species within the lattice, though the exact structure of these O_{2i} dimers has been the subject of considerable debate [4–6]. The results of *ab initio* calculations have led to the proposal

that two O atoms can be incorporated into neighbouring near-BC sites in either a staggered ($-\text{O}_i-\text{Si}-\text{O}_i-$) configuration or in a skewed ($-\text{O}_i-\text{Si}-\text{Si}-\text{O}_i-$) configuration [4–6]. Although the reports differ on the binding energy of the different arrangements, partly due to differences in the details of the calculations, it appears that the staggered dimer configuration is more favourable than the skewed dimer [4–6]. In addition to dimers, O interstitial trimers (O_{3i}) have also been examined both in a staggered chain and in a ring configuration. Results from calculations of the different trimer structures have shown that it is the staggered arrangement of chains of O atoms which tends to be more stable than a ring arrangement of Si and O atoms [4].

In addition to O_i and multi-oxygen centres, the structure and properties of the vacancy and multi-vacancy aggregates as well as vacancy–oxygen- (VO-) related defects are being continuously refined [7]. In disordered Si smaller multi-vacancy centres, such as the divacancy, tend to be present along with the VO centre [8]. However, in amorphized Si, larger multi-vacancies and open volume defects tend to be present. The early calculations of Chadi and Cheng [9] predicted the existence of a particularly stable multi-vacancy in the form of a puckered hexagonal ring, the ring hexavacancy, labelled V_6 . Further calculations, repeated at a more sophisticated level, confirmed this hypothesis and introduced the concept of ‘magic number’ multi-vacancies, such as V_6 and V_{10} [7, 10]. The predicted stability of the V_6 defect is due in part to a minimization of the number of Si dangling bonds and, upon reconstruction, results in the formation of a large void (~ 4.5 Å across) with trigonal (D_{3d}) symmetry. The V_6 centre has been predicted to be electrically inactive as well as possessing a small dipole moment, making it virtually undetectable in local mode infrared vibrational spectroscopy [10]. As a consequence, the V_6 centre and possible related configurations are an important class of defects in Si. It has been postulated, for example, that H-decorated V_6 centres are responsible for the 1.107 eV line emission [11] in Si and may also play a role in the formation of platelets [12]. Consequently, it is important to examine the possible structure(s) of V_6 -related centres which may be decorated with other atoms. One way that this can be accomplished is to make use of the partially shielded 4f electrons found in ions of the lanthanide series. These rare-earth ions are shielded from the full extent of the host crystal field by the closed 5s and 5p electron shells and this shielding effect has been exploited as a valuable probe for the study of point defects [13]. In this paper we wish to make use of Er^{3+} implanted into Si to probe the EPR complexes involving O. Extensive research on the Er-doped Si system has been performed since it is now well established as one of the most efficient ways to obtain light emission at the technologically important 1.5 μm wavelength. The addition of O (or other light atoms such as F) has shown that the room temperature luminescence can be enhanced and this has been attributed to the formation of Er–impurity complexes [14]. The presence of light atoms also helps with increased rare-earth incorporation in Si before the onset of silicide precipitation. It is thus important to examine the structure of these Si–O–Er centres not just to gain information relevant to the Si–Er system itself but for fundamental study of multi-oxygen-related defects in Si as well.

In a previous paper the results of EPR measurements made on Er- and O-coimplanted Si were reported [15]. This paper reported the presence of several Er^{3+} -related centres with monoclinic and trigonal symmetry. On the basis of comparison with known g -values from other systems, a tentative model for the monoclinic centre was proposed; no model for the centre which exhibited trigonal symmetry was presented. It is the intention of this paper to revisit the original EPR results in the light of recent calculations made on a number of relevant material systems. This paper is organized as follows. In section 2 a brief description of the samples used in the original study is presented and for convenience a summary of the main results and conclusions from the original EPR experiment is provided. The proposed different structures for the monoclinic and trigonal centres are then discussed in sections 3.1 and 3.2, respectively.

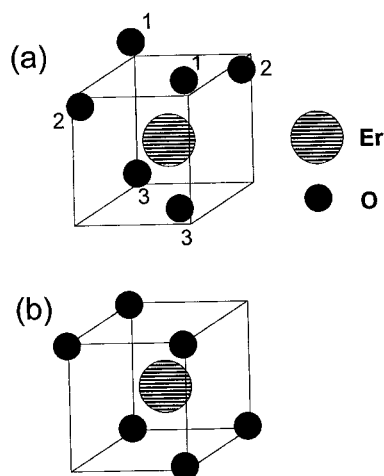


Figure 1. Arrangements of O atoms around a central Er atom found in (a) the monoclinic C_2 and (b) the trigonal C_{3i} configurations of the C phase of Er_2O_3 . In (a) the O atoms are not at equal distances from the Er ion and this is indicated by the O atoms not residing on the corners of the cube. Pairs of atoms at the same Er–O distance are indicated by 1, 2 and 3. In (b) all the Er–O distances are equal.

2. Summary of results

Multiple energy implants of Er to a dose of 10^{15} cm^{-2} were performed into float zone Si at 77 K, which resulted in a uniform concentration of $10^{19} \text{ Er cm}^{-3}$ extending nearly $2 \mu\text{m}$ below the surface. Some samples were coimplanted with O ions to achieve an average O concentration of 3×10^{19} or 10^{20} cm^{-3} overlapping with the Er concentration. The samples were then subsequently annealed at 450°C for 30 min and then 620°C for 3 h with some samples further annealed at 900°C for 30 s. The low-temperature EPR measurements were performed in a modified Bruker EPR spectrometer employing 100 kHz field modulation and at a microwave frequency of 9.23 GHz. From the samples with no O or with a 3:1 O:Er impurity ratio, no sharp EPR lines were observed. By contrast, from the sample with a 10:1 impurity ratio, sharp EPR lines were observed whether the sample was annealed to 620°C for 3 h only or had an additional 900°C anneal for 30 s. These sharp lines were shown to be associated with Er^{3+} centres with either monoclinic or trigonal symmetry and their g -values, along with the associated point symmetry, are reported in table 1. The appearance of these sharp lines as the O:Er concentration ratio increased from 3:1 to 10:1 implies that well defined Si–O–Er complexes with a high coordination number of O atoms have formed.

One centre, which exhibited monoclinic symmetry, labelled OEr-1, was attributed to an Er ion surrounded by six O atoms in a configuration similar to that found in the monoclinic configuration of Er-doped Y_2O_3 , which has the same structure as for Er_2O_3 [16]. The measured g -values for Er^{3+} in Y_2O_3 are also reported in table 1 [17]. The C phase of Er_2O_3 is known to occur with two different coordinations each of which consists of an Er^{3+} ion surrounded by six O atoms, though neither ErO_6 structure is in the form of an octahedron. The EPR measurements revealed Er to be in sites with monoclinic C_2 and trigonal C_{3i} (S_6) symmetry (cf table 1). In the case of the monoclinic centre the O–Er distances and the O–Er–O angles are not all equal, but come in three pairs as shown in figure 1. A second monoclinic centre, labelled OEr-3, was also reported in [15] and, in view of the similarities of the g -values and

Table 1. Principal g -values for different Er^{3+} -related centres.

Centre	g_1	g_2	g_3	Symmetry, τ (deg) ^a	g_{av}
OEr-1	0.80	5.45	12.55	Monoclinic, 56.9	6.27
OEr-2	0.69	3.24	3.24	Trigonal, 54.7	2.39
OEr-3	1.09	5.05	12.78	Monoclinic, 48.3	6.31
OEr-4	2.00	6.23	6.23	Trigonal, 54.7	4.82
Er_2O_3	1.64	4.89	12.31	Monoclinic	6.28
Er_2O_3	12.17	3.32	3.32	Trigonal	6.27

^a The angle τ is the angle by which the principal g_1 - and g_3 -axes in the Si–O–Er system are rotated about g_2 as measured relative to [001] and [010]. The direction of g_2 is along a [110] direction having being rotated by 45° from [100].

point symmetry of centre OEr-3 and centre OEr-1, these two centres are believed to have very similar structures. However, the exact arrangement of these defect complexes within the Si lattice was unknown. Two centres, labelled OEr-2 and OEr-4, which exhibited trigonal symmetry were also observed, though the intensity of centre OEr-2 was considerably higher than that of OEr-4. The g -values of these centres were sufficiently different from those of the trigonal centre found in erbium oxide and any other known Er^{3+} centre that no structures for these centres were proposed in the original study. The structure of these different centres will be discussed later, though the discussion will concentrate on centres OEr-1 and OEr-2.

Subsequent extended x-ray absorption fine-structure (EXAFS) measurements made on the same samples investigated by EPR confirmed the original hypothesis that the first coordination shell consisted of O [18]. It was found that in samples with an O:Er impurity ratio of 10:1, the average number of O atoms surrounding the Er atom was 5.1 ± 0.5 and the average Er–O separation was 2.26 Å, close to the average value found in erbium oxide (2.27 Å). It is important to realize that the EXAFS measurements probe the environment of all the Er ions (both divalent and trivalent), whereas the EPR results are from the EPR-active trivalent Er^{3+} centres. Consequently, the average number of 5.1 ± 0.5 O atoms surrounding the Er atom obtained in the EXAFS study indicates that there is a distribution of Si–O–Er centres present. The results from the EPR measurements therefore reflect a subset of all Er-related centres in the samples investigated.

3. Discussion of the structure of the Si–O–Er centres

3.1. Monoclinic centre

In order to analyse the g -values found in the Si–O–Er system, the crystal field experienced by the Er ion is taken, as a first approximation, to be cubic and on it a weaker lower-symmetry crystal field is superimposed. This is referred to as the cubic crystal field (CCF) approximation. If the magnitude of the non-cubic component of the crystal field is sufficiently small to be treated as a perturbation to the CCF, then the average of the trace of the g -tensor, g_{av} , as defined by

$$g_{av} = (1/3)(g_1 + g_2 + g_3), \quad (1)$$

is conserved and would equal the g -value found in cubic symmetry, g_c [19]. In this way the average g -value can be used as a quantitative measure of the local crystal field around a paramagnetic rare earth ion. This establishes the use of rare earth ions as probes of the local structure of defects in semiconductor and insulator materials. From table 1, it is evident that not only are the g -values of the centre OEr-1 (and OEr-3) similar to those found for Er-doped Y_2O_3 , but also g_{av} for OEr-1 is almost identical, at 6.27, to the average value found for the

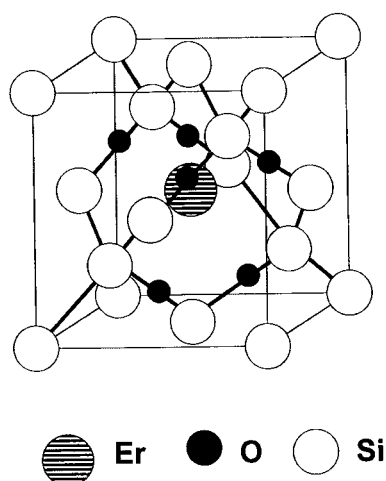


Figure 2. The proposed structure of centre OEr-1. The six O atoms surround the Er atom which is located at the tetrahedral interstitial site in Si. The O atoms are arranged in three sets of interstitial dimers. In the configuration presented, the O atoms are located at the BC positions, giving C_{2v} symmetry. By eliminating the C_2 axis of rotation, such as via a small movement of some of the O atoms away from the BC position, the symmetry is reduced to the observed C_{1h} .

oxide (6.28). It was on this basis that it was deduced that centre OEr-1 consists of six O atoms surrounding the Er ion in a manner similar to that found in the oxide, though this original assignment [16] failed to indicate how this ErO_6 complex was positioned within the lattice. Figure 2 now addresses this issue and shows the proposed structure of centre OEr-1. First, in order for this centre to possess the correct observed monoclinic C_{1h} symmetry the defect centre must exhibit a single plane of reflection corresponding to a $\{110\}$ plane of the Si lattice. The centre consists of an Er ion located at the tetrahedral interstitial site (T_i) surrounded by three sets of oxygen interstitial dimers. The O atoms in figure 2 have been located at exactly the BC positions, the significance of which will be discussed later. At any point surrounding the rare-earth ion the Si–O bonding arrangement can be viewed as $\cdots(\text{Si–O–Si–O–Si})\text{–}(\text{Si–O–Si–O–Si})\cdots$. The presence of the central Si–Si bond effectively isolates one dimer from the other dimers present. Such O incorporation is strongly driven since it is well known that the energy gained by breaking a single Si–Si bond and replacing it by two Si–O bonds is 7 eV, making O incorporation near to the BC position highly favourable. It was also established, in the case of the isolated staggered O_{2i} dimer, that the dimer structure is more stable than two single-interstitial O_i atoms by 0.2–0.6 eV [4, 6]. Locating the O atoms at exactly the BC positions results in an overall orthorhombic (C_{2v}) symmetry in which are present two $\{110\}$ mirror planes containing the C_2 axis of rotation. In order to lower the symmetry to the observed monoclinic C_{1h} symmetry it is simply a matter of removing the C_2 axis of rotation. This can be readily accomplished by moving some of the O atoms away from the exact BC positions to near to the BC site resulting in the Er–O separations no longer being equal to one another. This is directly analogous to the situation discussed earlier for the configuration of the monoclinic site found in Er_2O_3 (cf figure 1(a)). *Ab initio* calculations also favour such an O migration away from the BC site, since it was reported that a favoured configuration for O_{2i} dimers is for the Si–O–Si bond angle to be 131° , different from the 180° corresponding to the ideal BC position [4].

Secondly the T_i site was chosen for the location of the Er ion since it has been previously established, both experimentally, using emission channelling [20], and theoretically, using

ab initio calculations, that in O-free Si this is the most favoured position [21, 22]. The T_i site has sufficient space to accommodate the large Er ion and also does not result in breaking of Si–Si bonds. Furthermore, if the relaxation of the O atoms away from the BC positions is small, the Er–O separation should be approximately equal to the distance from the T_i site to the BC site (2.25 Å). This is close to the average Er–O separation (2.27 Å) found in the centres with monoclinic symmetry in Er_2O_3 [23]. To date there have been very few theoretical studies of the structure of the Si–O–Er centres. Recent first-principles calculations by Hashimoto and others [24] have attempted to determine the most stable atomic configurations of the ErO_6 system. They calculated the formation energies of a number of different ErO_6 configurations in Si and found that the two lowest-energy structures had orthorhombic (C_{2v}) and monoclinic (C_2) symmetry. The structure of the centre with C_{2v} symmetry is similar to that discussed above, whilst the centre with C_2 symmetry was observed to be 0.44 eV higher in energy than the orthorhombic centre. They also considered the effects of relaxing this structure and found a more relaxed C_{2v} state similar to that associated with centre OEr-1. In summary, the structure proposed in figure 2 explains not only the magnitude and the average of the observed g -values, but also the point symmetry around the Er^{3+} ion as measured by means of EPR. The structure is simultaneously mimicking the local structure of the monoclinic site in Er_2O_3 , as well as gaining energy through the breaking of Si–Si bonds and replacement of them by strong Si–O bonds with the O atoms near the BC positions.

3.2. Trigonal centre

The discussion of the structure of the monoclinic centres was based on comparison with the known structure and g -values for the corresponding low-symmetry centre found in Er-doped Y_2O_3 . Likewise it is possible to begin the discussion of the dominant trigonal centre, OEr-2, found in the Si–O–Er system by comparing it with the trigonal centre found in the oxide (figure 1(b)). From table 1, the g -values of the trigonal C_{3i} centre observed in $\text{Y}_2\text{O}_3:\text{Er}^{3+}$ are clearly different (with $g_{\parallel} > g_{\perp}$) from the g -values found for the OEr-2 centre ($g_{\parallel} < g_{\perp}$). Note that in both cases, however, the values of g_{\perp} are almost the same, with $g_{\perp} = 3.24$ for the Si–O–Er system and $g_{\perp} = 3.32$ for the oxide. The major difference between the two centres is found in the value of g_{\parallel} . This may indicate that the crystal field around the Er ion and hence the local structure around the Er ion in the plane perpendicular to the trigonal defect axis are similar [25]. To conclusively prove that a particular structure is associated with a particular EPR centre, a thorough *ab initio* study would have to be performed. Since this is beyond the scope of this paper, we first explore the magnetic resonance analysis for a centre with cubic symmetry and then extend the analysis to the case of trigonal symmetry. In the case of Er^{3+} in cubic symmetry, the different irreducible representations can be readily obtained from group theory and can be represented by $\Gamma_6 + \Gamma_7 + 3\Gamma_8$. The Γ_6 and Γ_7 irreducible representations of the cubic group are twofold degenerate and each of the three Γ_8 levels is fourfold degenerate. For each of the cubic irreducible representations Γ_6 , Γ_7 and Γ_8 , the values of m_J in the eigenvector expansion will differ by four to reflect the presence of a fourfold axis of rotational symmetry. In such a situation the CCF approximation, and hence the corresponding CCF eigenstates, can be employed, in which the cubic rare-earth crystal field Hamiltonian [26] can be expressed as

$$H = B_4(O_4^0 + 5O_4^4) + B_6(O_6^0 - 21O_6^4), \quad (2)$$

where O_n^m are the crystal field equivalent operators and the coefficients B_4 and B_6 determine the crystal field splitting. Equation (2) can be solved through the introduction of two parameters x and W defined such that

$$B_4F(4) = Wx \quad \text{and} \quad B_6F(6) = W(1 - |x|), \quad (3)$$

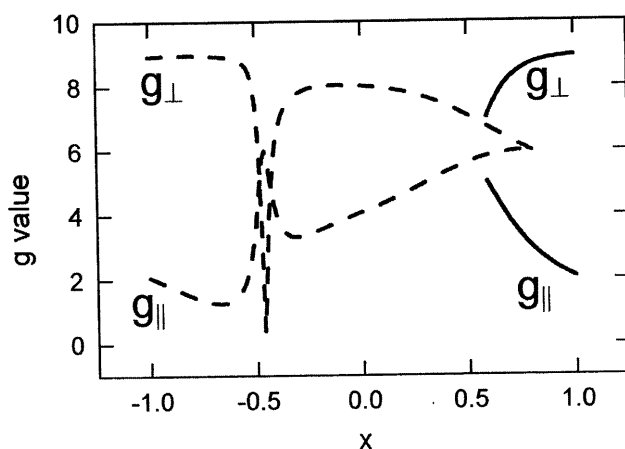


Figure 3. Calculated principal g -values for an Er^{3+} ion in a site of trigonal symmetry for $W > 0$ (solid curves) and $W < 0$ (dashed curves). The calculation assumes that the trigonal field is small so that cubic eigenstates can be used. Close to $x = -0.5$ it is observed that g_{\perp} becomes close to zero.

where W is an energy scale factor that depends on the electrostatic potentials and $F(4)$ and $F(6)$ are numerical constants [26]. The quantity x is the crystal field mixing term ($\sim B_4/B_6$) and runs from -1 to $+1$. With labelling appropriate to T_d symmetry, the Γ_7 representation lies lowest for $-1 < x < -0.46$, the Γ_6 representation for $-0.46 < x < 0.58$ and the Γ_8 representation for $x > 0.58$. From the crystal field eigenstates, the g -values associated with transitions within the Γ_6 and Γ_7 states are 6.80 and 6.00 and are independent of x . For centres with less than cubic symmetry it is possible to use equation (1) to relate the observed principal g -values to the g -value associated with a centre with cubic symmetry, g_c [19]. Since the average g -value for centre OEr-2 is 2.39 and is far enough removed from the cubic g -values for a Γ_6 state (6.8) or Γ_7 state (6.0), we can conclude that this centre is not associated with an Er^{3+} ion surrounded by four tetrahedrally arranged O atoms for which $x < 0$. Neither can this centre be associated with an environment of six octahedrally coordinated O atoms for which $0 < x < 0.58$. For the remaining region of $0.58 < x < 1$ (also associated with octahedral coordination), corresponding to a Γ_8 level lying lowest, the use of the average g -value is not valid. This is also the case for $W < 0$ for $-1 < x < 0.8$. In this case it is necessary to calculate the g -values for each value of x and use the associated CCF eigenstates, labelled P and Q in the notation of [19], to calculate the principal g -values g_{\parallel} and g_{\perp} via

$$g_{\parallel} = g_J(P - Q) \quad \text{and} \quad g_{\perp} = g_J(P + Q). \quad (4)$$

where the Landé g -value is taken to be $6/5$. Figure 3 shows the calculated g -values determined by this method using intervals for x of 0.01 for both $W > 0$ and $W < 0$. It is evident from figure 3 that no unique value of x exists for which the calculated values of g_{\parallel} approach the observed value of 0.69 and g_{\perp} approaches 3.24; we therefore conclude that centre OEr-2 does not originate from a trigonally split Γ_8 ground state. The overall result is that centre OEr-2 cannot be associated with an Er^{3+} ion in either tetrahedral or octahedral O coordination.

Since simple octahedral oxygen coordination has been ruled out as a possible explanation for centre OEr-2, alternative models are required. It is possible to adapt the three O_{2i} -dimer model presented in figure 2 by rearrangement of some of the O atoms to different (near-) BC positions to give overall trigonal symmetry as shown in figure 4. In this configuration the

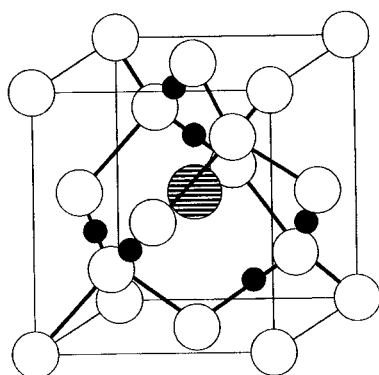


Figure 4. A possible structure for centre OEr-2 using three O_{21} dimers. The Er atom is located at the T_i site and the Er–O distances are all equal to each other. The overall symmetry is C_3 .

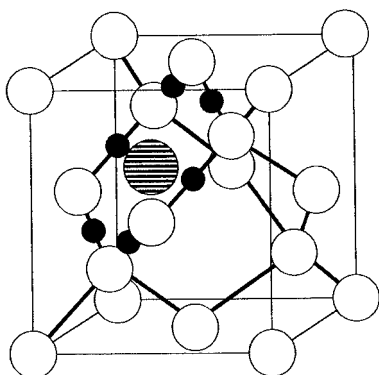


Figure 5. A possible structure for centre OEr-2 with the Er atom located at the hexagonal interstitial site and each of the Si–Si bonds in the hexagonal ring replaced by two Si–O bonds. The O atoms are located exactly at BC positions and the overall symmetry is D_{3d} .

Er–O separations are all equal and the overall symmetry is C_3 . The dimers are again separated by Si–Si bonds as in the model proposed for the monoclinic centre. However, the *ab initio* calculations of Hashimoto *et al* [24] showed that this structure was 2.42 eV less stable than the structure of the centres investigated and consequently it is not believed that this is the structure of the OEr-2 trigonal centre.

Other atomic positions and coordinations therefore need to be considered. There exist a number of other positions for impurity atoms in the Si lattice which can give rise to trigonal symmetry. Two such sites are defects located at the BC position and also the hexagonal interstitial (H_i) position. Locating an Er atom at the BC site would result in the formation of two Er–Si bonds with the nearest neighbours being Si rather than O atoms. Furthermore, in order to accommodate a large number of O atoms a large defect centre is desirable. Figure 5 shows the arrangement of atoms at the hexagonal interstitial site in which each nearby Si–Si bond has been replaced by two Si–O bonds with the O atoms located exactly at the BC sites and the Er^{3+} ion located at the H_i site. In Si, the distance from the H_i site to the BC site is only 1.92 Å and that to the unrelaxed Si is 2.25 Å. Although this arrangement of atoms has trigonal D_{3d} point symmetry and is consistent with the magnetic resonance data, it is not believed to be the optimal

arrangement of centre OEr-2 for two reasons. First, in the atomic arrangement of figure 5 the bonding around the hexagonal ring alternates evenly between Si and O atoms with each O atom being shared between two Si atoms. The calculations of Pesola *et al* [4] examined the formation and binding energies when placing three O atoms in a ring arrangement or in a staggered arrangement. Both of these configurations also had alternate Si–O bonding. They noted that for these arrangements there was a stronger tendency for the O atoms to prefer to form the staggered chains rather than a ring arrangement. Pesola *et al* also found that the ring configuration of O_{3i} is stabilized by only 0.2 eV when compared to splitting into three O_i, whereas the corresponding binding energy for the staggered chain was 0.7 eV against splitting into three O_i atoms. Consequently, such ring arrangements are believed to be less stable than chain arrangements.

Secondly, as O aggregation in the ring increases, incorporation of the six O atoms required in figure 5 will result in an increase in the strain energy in the ring until it becomes energetically favourable for a VO_n complex to form, with the release of a Si self-interstitial (Si_i). The maximum size of O_{ni} can be estimated as follows; taking the formation energy of Si_i to be 4.2 eV, and using the formation energies quoted by Pesola *et al* of 1.1 eV for O_i and 3.7 eV for a VO centre, the reaction O_i → VO + Si_i is seen to be highly endothermic, requiring over 6.8 eV. Since the formation energy of the silicon interstitial is constant, the relative difference between the formation energies of interstitial oxygen and the VO centre is only 2.6 eV. This reduces to 1.6 eV for the case of the O_{2i} dimer for which Pesola quotes formation energies of 2.1 and 3.7 eV for O_{2i} and VO₂, respectively. This reduction in the energy difference between O_{ni} and VO_n as the number of O atoms increases will ultimately result in the reaction O_{ni} → VO_n + Si_i becoming exothermic before the six-atom O hexamer will form. This proposition has been recently confirmed by Jones *et al* [27], who show that the reaction for the kick-out of the Si_i and the formation of VO_n becomes exothermic for *n* equal to four.

We propose an alternative model that is stable against the dissolution of the Si–O rings, consistent with the EPR results and is based on the H_i site model discussed above. The model proposed reflects the likelihood of a high number of vacancy and multi-vacancy centres being produced by MeV ion implantation. In this model, shown in figure 6, the Er atom is placed in the centre of a ring hexavacancy decorated by six O atoms. In the ideal geometry of the undecorated V₆ centre, 12 Si atoms are the nearest-neighbour atoms of the vacant sites, such that each pair of atoms shares a single vacant site. Pairs of Si atoms are displaced toward each other to form a weak reconstructed Si–Si bond. A total of six Si–Si reconstructed bonds each with a bond length of around 2.6 Å forms [7]. After reconstruction, V₆ possesses trigonal D_{3d} symmetry with an idealized distance across the defect of 4.5 Å. The model proposes that the O atoms enter into or near to the centre of the reconstructed bonds, effectively producing six Si–O–Si bonds, but unlike in the H_i site model described earlier, they are effectively isolated from each other. Examination of figure 6 shows that the bonding arrangement is Si–O–Si–Si–O–Si, which will minimize the O–O interaction and allow electrons to be gathered from the Si and from the Er by O. This model is also consistent with the trigonal symmetry observed in the EPR measurements. In this model the atomic arrangement along the defect axis consists of two pairs of reconstructed Si–Si bonds and the Er ion. A decorated hexavacancy-related centre is plausible in these materials, considering the non-equilibrium method of Er and O incorporation (ion implantation) into the Si.

The decorated hexavacancy model previously discussed is not just confined to the case of rare-earth incorporation. MeV ion implantation which generates large quantities of multi-vacancy centres may act as gettering centres for metal atoms. Estreicher has modelled the situation of Cu incorporation into Si containing V₆ centres and reported multi-decoration of the V₆ centres with Cu ions [28]. Whether the formation of a decorated ring hexavacancy occurs will depend on whether the vacancy centres are stable upon annealing. This in turn

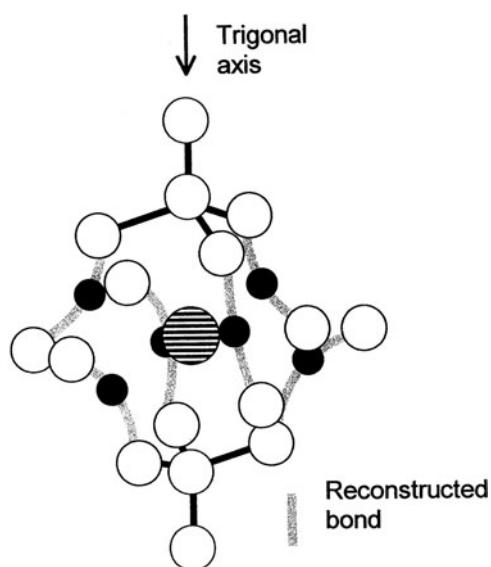


Figure 6. A possible structure for centre OEr-2 with the Er atom located at the centre of an O-decorated ring hexavacancy centre. Each of the reconstructed Si-Si bonds in then replaced by two Si-O bonds. The overall symmetry is D_{3d} .

will be affected by the presence of strong metal gettering centres and whether the presence of O atoms is able to break the reconstructed Si-Si bonds forming strong Si-O-Si bonds. In this way the O-decorated ring hexavacancy can be formed by ion implantation of MeV heavy ions into Si in the presence of O atoms.

4. Conclusions

In conclusion, different models for multi-O-related centres in Si formed by incorporation of the rare-earth ion erbium are explored. In the case of a centre exhibiting monoclinic symmetry, the structure of the centre is explained in terms of six O atoms arranged around an Er^{3+} ion located at the T_i site in the Si lattice. The O atoms are grouped into three dimers with the O atoms near to BC positions. In this way, the proposed structure is consistent with the observed g -values as well as the point symmetry as measured by means of EPR. The centre is stabilized through the breaking of Si-Si bonds and replacement of them with strong Si-O bonds in which the Er-O separation is close to that found in the erbium oxide. Three possible models for the observed trigonal centre were examined, including a variation of the monoclinic centre, a centre based on Er located at the hexagonal interstitial site and thirdly a model in which the Er atom is at the centre of an O-decorated ring hexavacancy centre. The structure of the different centres was examined in each case and the relevance to the study of defects in MeV high-dose implantation into Si considered.

References

- [1] Jones R and Briddon P R 1998 Identification of defects in semiconductors *Semiconductor and Semimetals* vol 51A, ed M Stavola (Boston, MA: Academic) ch 6
- [2] Newman R C 2000 *J. Phys.: Condens. Matter* **12** R335
- [3] Pesola M, Von Boehm J and Nieminen R M 1999 *Phys. Rev. Lett.* **82** 4022

- [4] Pesola M, Von Boehm J, Mattila T and Nieminen R M 1999 *Phys. Rev. B* **60** 11 449
- [5] Needels M, Joannopoulos J D, Bar-Yam Y and Pantelides S T 1999 *Phys. Rev. B* **43** 5375
- [6] Coutinho J, Jones R, Briddon P R and Oberg S 2000 *Phys. Rev. B* **62** 10 824
- [7] Hastings J L, Estreicher S K and Fedders P A 1997 *Phys. Rev. B* **56** 10 215
- [8] Amarendra G, Rajaraman R, Venugopal Rao G, Nair K G M, Viswanathan B, Suzuki R, Ohdaira T and Mikado T 2001 *Phys. Rev. B* **63** 224112
- [9] Chadi D J and Chang K J 1988 *Phys. Rev. B* **38** 1523
- [10] Estreicher S K, Hastings J L and Fedders P A 1997 *Appl. Phys. Lett.* **70** 432
- [11] Hourahine B, Jones R, Safonov A N, Oberg S, Briddon P R and Estreicher S K 2000 *Phys. Rev. B* **61** 12 594
- [12] Mori T, Otsuka K, Umehara N, Ishioka K, Kitajima M, Hishita S and Murakami K 2001 *Physica B* **302** 239
- [13] Polman A 2001 *Physica B* **300** 78
- [14] Priolo F, Franzò G, Coffa S, Polman A, Libertino S, Barklie R and Carey D 1995 *J. Appl. Phys.* **78** 3874
- [15] Carey J D, Barklie R C, Donegan J F, Priolo F, Franzò G and Coffa S 1999 *Phys. Rev. B* **59** 2773
- [16] Carey J D, Donegan J F, Barklie R C, Priolo F, Franzò G and Coffa S 1996 *Appl. Phys. Lett.* **69** 3854
- [17] Schafer G and Scheller S 1966 *Phys. Kondens. Mater.* **5** 48
- [18] Terrasi A, Franzò G, Coffa S, Priolo F, D'Acapito F and Mobilio S 1997 *Appl. Phys. Lett.* **70** 1712
- [19] Abragam A and Bleaney B 1970 *Electron Paramagnetic Resonance Ions* (Oxford: Oxford University Press) p 720
- [20] Wahl U, Vantomme A, De Wachter J, Moons R, Langouche G, Marques J G and Correia J G (ISOLDE Collaboration) 1997 *Phys. Rev. Lett.* **79** 2069
- [21] Needles M, Schluter M and Lannoo M 1993 *Phys. Rev.* **47** 15 533
- [22] Wan J, Ling Y, Sun Q and Wang X 1998 *Phys. Rev. B* **58** 10 415
- [23] Moon R M, Koehler W C, Child H R and Raubenheimer L J 1968 *Phys. Rev.* **176** 722
- [24] Hashimoto M, Yanase A, Harima H and Katayama-Yoshida H 2001 *Physica B* **308–310** 378
- [25] When the magnetic field is perpendicular to the z -axis, the effects of the additional trigonal crystal field components (O_4^3 and O_6^3) disappear; see Abragam A and Bleaney B 1970 *Electron Paramagnetic Resonance Ions* (Oxford: Oxford University Press) p 338
- [26] Lea K R, Leask M J M and Wolf W P 1962 *J. Phys. Chem. Solids* **23** 1381
- [27] Jones R, Coutinho J, Oberg S and Briddon P R 2001 *Physica B* **308–310** 8
- [28] Estreicher S K 1999 *Phys. Rev. B* **60** 5375